

Novel 1-D Chains Constructed of Rings Which Include Six Metal Atoms [M₂Au₄] (M = Ni, Zn) with Auophilic Interactions: Structure, Magnetic, and Spectral Studies

by Shu-Ping Wang^a), You Song^b), Dong-Zhao Gao^a), Li-Cun Li^a), Qing-Mei Wang^a), Dai-Zheng Liao^a), Zong-Hui Jiang^{*a}b), and Shi-Ping Yan^a)

^a) Department of Chemistry, Nankai University, Tianjin 300071, P. R. China
(fax: +86 22 23 50 27 79; e-mail: coord@nankai.edu.cn)

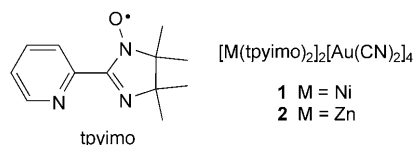
^b) State Key Laboratory of Coordination Chemistry, Nanjing University, Nanjing 210093, P. R. China

Two novel 1-D chain complexes of a formal iminomethyl nitroxide radical [M(tpyimo)₂]₂[Au(CN)₂]₄ (M = Ni, Zn for **1** and **2**, tpyimo = 4,5-dihydro-4,4,5,5-tetramethyl-2-(pyridin-2-yl)-1*H*-imidazol-1-yloxy), were synthesized and structurally characterized. Both 1-D chains consist of two kinds of chair-conformation rings, which include six metal atoms [M₂Au₄] (M = Ni, Zn), and are connected to each other alternately through auophilic interactions. On the other hand, [Au(CN)₂]₄ oligomers are also formed through auophilic interactions, and used as bridges in the 1-D chains. The magnetic coupling between the Ni^{II} ion and the tpyimo radical in **1** is a strong ferromagnetic interaction. Strong ligand-centered luminescence is observed at room temperature for both complexes.

Introduction. – The design of multidimensional supramolecular assemblies is an area of intense current interests [1–3]. This is due not only to their potential applications in electrical conductivity, molecule-based magnets, molecular absorption, ion exchange, heterogeneous catalysis, *etc.*, but also to their intriguing structural diversity [4–11]. Gold(I) has stimulated great interest for its tendency to aggregate through closed shell ‘auophilic’ interaction and the consequent luminescence properties [12–16]. The supramolecular chemistry is replete with these polymeric systems of Au^I by virtue of the Au–Au interactions. [Au(CN)₂][–] aggregates under a variety of conditions in its compounds, and most of them display fascinating spectroscopic properties [17–23]. Their luminescence properties are attributed to auophilic interaction in these studies.

On the other hand, nitroxide radicals are useful paramagnetic building blocks, which offer opportunities to design multidimensional and multispin systems. They have been used to design many new functional complexes associated with a variety of structural topology and particular physical properties [24–34].

However, the studies dealing with both Au^I and nitroxide radicals are rather limited [35]. Taking advantage of both the Au^I compounds and nitroxide-radical ligands, we now present two (iminomethyl nitroxide)metal complexes **1** and **2** with [Au(CN)₂][–] as coligands, the iminomethyl nitroxide being 4,5-dihydro-4,4,5,5-tetramethyl-2-(pyridin-2-yl)-1*H*-imidazol-1-yloxy (tpyimo). Both complexes are 1-D chain complexes with a particular structure, in which the chain is constructed of hexametal rings with auophilic interactions. Their interesting magnetic and luminescence properties were also studied.



Result and Discussion. – *Crystal Structures.* The crystallization of complexes **1** and **2** from MeOH/H₂O gave single crystals with the formula $[\text{M}(\text{tpyimo})_2][\text{Au}(\text{CN})_2]_4 \cdot 6 \text{H}_2\text{O} \cdot 0.75 \text{MeOH}$ as a crystallographic repeating unit. Both crystals are solvates and contain H₂O molecules and MeOH molecules. They crystallize in an isomorphous monoclinic space group $P2_1/c$ with $Z=4$ (see *Table 1* for crystal data and details of the structure determinations). Selected bond lengths and angles are listed in *Table 2* for **1** and in *Table 3* for **2**. Disorders and/or thermal motions were observed for partial cyanide groups (C(7)–N(7)) and solvent H₂O and MeOH molecules. The structure of $[\text{Ni}(\text{tpyimo})_2][\text{Au}(\text{CN})_2]_4$ unit of **1** is shown in *Fig. 1*. There are two independent central Ni^{II} ions, Ni(1) and Ni(2), in one unit. The coordination geometry around the two Ni^{II} ions are similar, which both are distorted octahedrons (NiN₆) and can be described as *cis*(CN)-*trans*(py) isomers with slightly different bond parameters. The tpyimo coordinates to one Ni^{II} ion *via* the pyridinyl and imino N-atoms to form a planar five-member chelate ring as found in $[\text{MCl}_2(\text{tpyimo})_2]$ (M=Mn, Co, Ni, Zn) [36]. The chelate ring is almost coplanar not only to the pyridinyl ring but also to the iminomethyl nitroxide moiety. Two $[\text{Au}(\text{CN})_2]^-$ anions are linked to the $[\text{Ni}(\text{tpyimo})_2]^{2+}$ unit in '*cis*'-configuration. The crystal structures consist of infinite 1-D zigzag polymeric chains of $[\text{Ni}(\text{tpyimo})_2][\text{Au}(\text{CN})_2]_4$ with $[\text{Au}(\text{CN})_2]^-$ oligomers as bridges (*Fig. 2*). Each $[\text{Au}(\text{CN})_2]^-$ oligomer (Au(3)–Au(1)–Au(2)–Au(4)) is composed of four $\text{Au}(\text{CN})_2^-$ anions through aurophilic interactions (the Au–Au distances, 3.260(2) to 3.339(1) Å, are much shorter than the sum of the *van der Waals* radii of Au, 3.60 Å). In every $[\text{Au}(\text{CN})_2]^-$ anion, one CN[−] group is used as a bridging ligand between the Ni^{II} and Au^I ion, another is a terminal ligand of the Au^I ion, which is consistent with the IR results. The overall framework of the 1D zig-zag chain consists of two kinds of independent chair-conformation hexametal rings (*Fig. 2*), which are connected to each other alternately through aurophilic interactions (Au(1)–Au(2)). The shortest intermolecular N–O⋯O–N contacts of 3.227 Å occur between interchain-uncoordinated nitroxide groups of tpyimo. The structure characteristics of **2** are very similar to that of **1**, except for slight differences in the crystal data and bond parameters. Noteworthy, aurophilic interactions facilitate the formation of $[\text{Au}(\text{CN})_2]^-$ oligomer bridges and 1-D zig-zag chains in both complexes.

IR Spectra. Both complexes **1** and **2** show two sharp $\tilde{\nu}$ bands at *ca.* 2150 and 2184 cm^{−1}, which can be attributed to the C≡N stretching vibration. The splitting of $\tilde{\nu}(\text{CN})$ indicates the presence of two different coordination modes (terminal and bridging) of the CN[−] ligands. It is well known that the formation of a CN[−] bridge shifts $\tilde{\nu}(\text{CN})$ toward higher frequencies [37–40]. The strong band at 2184 cm^{−1} may, therefore, be attributed to $\tilde{\nu}(\text{CN})$ of the bridging CN[−] and that at 2150 cm^{−1} to the terminal ones. The characteristic $\tilde{\nu}(\text{NO})$ vibration of tpyimo appears at 1373 cm^{−1}.

Magnetic Properties. The plots of $\chi_M T$ vs. T and χ_M^{-1} vs. T for complex **1** is shown in *Fig. 3*. The χ_M is the magnetic susceptibility per $[\text{Ni}(\text{tpyimo})_2][\text{Au}(\text{CN})_2]_2$ unit. Consid-

Table 1. Crystal Data and Details of Structural Determination of Complexes **1** and **2**

	1	2
Empirical formula	C _{56.75} H ₇₉ Au ₄ Ni ₂ N ₂₀ O _{10.75}	C _{56.75} H ₇₉ Au ₄ Zn ₂ N ₂₀ O _{10.75}
M_r	2118.69	2132.01
Crystal system	monoclinic	monoclinic
Space group	$P2_1/c$	$P2_1/c$
a [Å]	22.211(9)	22.265(6)
b [Å]	17.457(7)	17.506(5)
c [Å]	19.726(8)	19.738(5)
β [°]	93.862(7)	93.671(5)
V [Å ³]	7631(5)	7678(4)
Z	4	4
μ (MoK α) [mm ⁻¹]	8.207	8.292
$F(000)$	4070	4086
θ Range [°]	0.92 to 25.01	0.92 to 26.43
Limiting indices	$-26 \leq h \leq 26, -20 \leq k \leq 18, -19 \leq l \leq 23$	$-24 \leq h \leq 27, -21 \leq k \leq 19, -24 \leq l \leq 22$
Total reflections	38948	36002
Unique reflections	13449	15667
R (int)	0.1276	0.1179
Data, restraints, parameters	13449, 350, 944	15667, 332, 936
Final R indices ($I > 2\sigma(I)$)	0.0764, 0.1412	0.0730, 0.1354
R indices (all data)	0.2101, 0.1966	0.2201, 0.1871
Goodness-of-fit on F^2	1.035	0.980
Largest diff. peak and hole [e Å ⁻³]	2.267, -1.885	1.826, -1.842

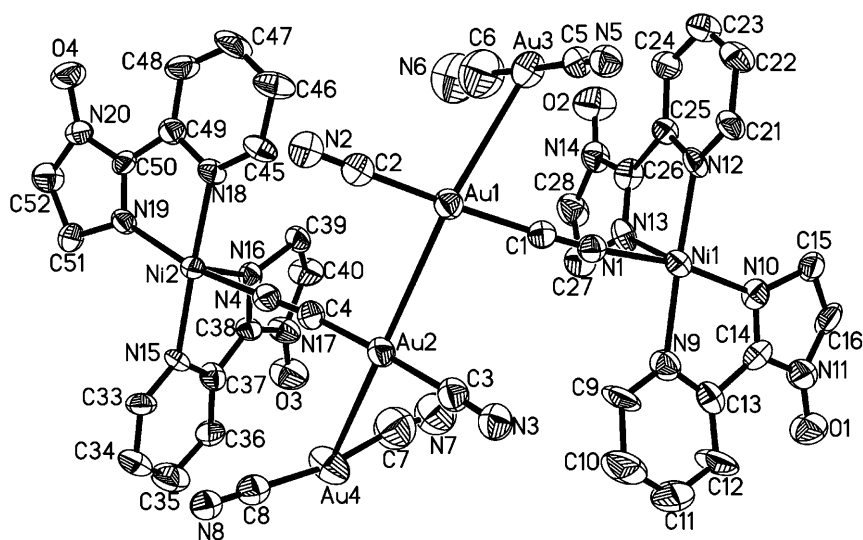


Fig. 1. Perspective drawing of the $[Ni(tpyimo)_2]_2[Au(CN)_2]_4$ repeat unit of **1** with 30% thermal ellipsoids. The Me groups of tpyimo are omitted for clarity.

Table 2. Selected Bond Lengths [Å] and Angles [°] of **1**

Au(1)–C(1)	2.03(2)	Au(1)–C(2)	1.97(2)
Au(2)–C(3)	1.98(2)	Au(2)–C(4)	1.94(2)
Au(3)–C(5)	1.98(2)	Au(3)–C(6)	1.90(4)
Au(4)–C(7)	2.006(9)	Au(4)–C(8)	1.93(2)
Ni(1)–N(5)#1 ^a	2.05(2)	Ni(1)–N(1)	2.07(2)
Ni(1)–N(12)	2.09(2)	Ni(1)–N(9)	2.096(2)
Ni(1)–N(13)	2.10(2)	Ni(1)–N(10)	2.14(2)
Ni(2)–N(4)	2.04(2)	Ni(2)–N(8)#2	2.05(2)
Ni(2)–N(18)	2.11(1)	Ni(2)–N(15)	2.12(1)
Ni(2)–N(16)	2.12(2)	Ni(2)–N(19)	2.13(1)
Au(1)–Au(3)	3.264(2)	Au(1)–Au(2)	3.339(1)
Au(2)–Au(4)	3.260(2)		
C(2)–Au(1)–C(1)	177.0(8)	Au(3)–Au(1)–Au(2)	148.64(4)
C(4)–Au(2)–C(3)	176.9(8)	Au(4)–Au(2)–Au(1)	160.71(4)
C(6)–Au(3)–C(5)	178(1)	C(8)–Au(4)–C(7)	170(2)
N(5)#1–Ni(1)–N(13) ^a	171.0(7)	N(1)–Ni(1)–N(10)	169.6(6)
N(12)–Ni(1)–N(9)	177.3(7)	N(5)#1–Ni(1)–N(9) ^a	87.4(6)
N(5)#1–Ni(1)–N(10) ^a	91.5(6)	N(5)#1–Ni(1)–N(1) ^a	92.3(6)
N(5)#1–Ni(1)–N(12) ^a	92.6(6)	N(13)–Ni(1)–N(9)	101.6(7)
N(13)–Ni(1)–N(10)	91.2(6)	N(13)–Ni(1)–N(1)	86.5(6)
N(13)–Ni(1)–N(12)	78.4(6)	N(1)–Ni(1)–N(9)	92.8(6)
N(9)–Ni(1)–N(10)	77.7(7)	N(1)–Ni(1)–N(12)	89.9(6)
N(12)–Ni(1)–N(10)	99.6(6)	N(8)#2–Ni(2)–N(16) ^a	168.6(6)
N(18)–Ni(2)–N(15)	175.2(6)	N(4)–Ni(2)–N(19)	169.6(6)
N(8)#2–Ni(2)–N(4) ^a	91.7(6)	N(8)#2–Ni(2)–N(18) ^a	93.0(6)
N(8)#2–Ni(2)–N(15) ^a	91.6(6)	N(8)#2–Ni(2)–N(19) ^a	88.8(6)
N(16)–Ni(2)–N(4)	90.1(6)	N(16)–Ni(2)–N(18)	98.2(6)
N(16)–Ni(2)–N(15)	77.2(6)	N(16)–Ni(2)–N(19)	91.4(6)
N(4)–Ni(2)–N(18)	91.1(6)	N(4)–Ni(2)–N(15)	90.1(5)
N(18)–Ni(2)–N(19)	78.5(6)	N(15)–Ni(2)–N(19)	100.3(6)

^a) Symmetry transformations used to generate equivalent atoms: #1 = $-x+2, -y, -z+1$ and #2 = $-x+1, -y, -z+1$.

ering the structural characteristics, two independent Ni(tpyimo)₂ moieties were well isolated in the asymmetric [Ni(tpyimo)₂]₂[Au(CN)₂]₄ unit. So the magnetic data were interpreted considering only isolated Ni(tpyimo)₂ units involving one Ni^{II} ion.

The $\chi_M T$ value for **1** first increases from 2.67 cm³ K mol⁻¹ at room temperature to 3.06 cm³ K mol⁻¹ at 65 K, and then decreases sharply to 2.45 cm³ K mol⁻¹ at 2 K. The $\chi_M T$ value at room temperature is much higher than that expected for independent spins (1.75 cm³ K mol⁻¹ for one $S_{\text{Ni}}=1$ and two $S_{\text{Rad}}=1/2$), and the maximum value of $\chi_M T$ at 65 K is close to that expected for $S=2$ independent spins (3.00 cm³ K mol⁻¹). These magnetic behaviors suggest ferromagnetic couplings between Ni^{II} and tpyimo. To evaluate the exchange coupling constant in such a system, it was treated as a simplified three-spin model Rad-Ni^{II}-Rad with the Hamiltonian $\hat{H} = -2J(\hat{S}_{\text{Ni}} \cdot \hat{S}_{\text{rad1}} + \hat{S}_{\text{Ni}} \cdot \hat{S}_{\text{rad2}})$. The magnetic susceptibility expression is given by Eqn. 1 with exchange coupling constant ($2J$) between Ni^{II} and the tpyimo ligand. For the sharp decrease of the $\chi_M T$ value at low temperature, a molecular field approximation was included with the three-spin model.

Table 3. Selected Bond Lengths [Å] and Angles [°] of **2**

Au(1)–C(1)	1.97(2)	Au(1)–C(2)	1.91(2)
Au(2)–C(3)	1.98(2)	Au(2)–C(4)	1.96(2)
Au(3)–C(5)	1.97(2)	Au(3)–C(6)	1.95(3)
Au(4)–C(7)	2.006(9)	Au(4)–C(8)	1.99(2)
Zn(1)–N(5)#1 ^a	2.14(2)	Zn(1)–N(1)	2.13(2)
Zn(1)–N(12)	2.18(1)	Zn(1)–N(9)	2.13(1)
Zn(1)–N(13)	2.20(1)	Zn(1)–N(10)	2.24(1)
Zn(2)–N(4)	2.11(1)	Zn(2)–N(8)#2 ^a	2.10(2)
Zn(2)–N(18)	2.18(1)	Zn(2)–N(15)	2.19(1)
Zn(2)–N(16)	2.21(1)	Zn(2)–N(19)	2.19(1)
Au(1)–Au(3)	3.283(1)	Au(1)–Au(2)	3.293(1)
Au(2)–Au(4)	3.230(1)		
C(2)–Au(1)–C(1)	175.6(7)	Au(3)–Au(1)–Au(2)	146.55(3)
C(4)–Au(2)–C(3)	177.1(7)	Au(4)–Au(2)–Au(1)	159.12(3)
C(6)–Au(3)–C(5)	179(1)	C(8)–Au(4)–C(7)	169(2)
N(5)#1–Zn(1)–N(13) ^a	166.8(5)	N(1)–Zn(1)–N(10)	167.0(5)
N(12)–Zn(1)–N(9)	173.9(5)	N(5)#1–Zn(1)–N(9) ^a	90.2(5)
N(5)#1–Zn(1)–N(10) ^a	93.4(5)	N(5)#1–Zn(1)–N(1) ^a	92.8(5)
N(5)#1–Zn(1)–N(12) ^a	91.8(5)	N(13)–Zn(1)–N(9)	103.0(5)
N(13)–Zn(1)–N(10)	90.5(5)	N(13)–Zn(1)–N(1)	86.0(5)
N(13)–Zn(1)–N(12)	75.2(5)	N(1)–Zn(1)–N(9)	92.7(6)
N(9)–Zn(1)–N(10)	75.9(6)	N(1)–Zn(1)–N(12)	93.0(5)
N(12)–Zn(1)–N(10)	98.2(5)	N(8)#2–Zn(2)–N(16) ^a	166.0(5)
N(18)–Zn(2)–N(15)	171.9(5)	N(4)–Zn(2)–N(19)	165.2(5)
N(8)#2–Zn(2)–N(4) ^a	93.3(6)	N(8)#2–Zn(2)–N(18) ^a	95.8(5)
N(8)#2–Zn(2)–N(15) ^a	91.4(6)	N(8)#2–Zn(2)–N(19) ^a	88.8(5)
N(16)–Zn(2)–N(4)	90.8(5)	N(16)–Zn(2)–N(18)	97.6(5)
N(16)–Zn(2)–N(15)	75.0(5)	N(16)–Zn(2)–N(19)	90.6(5)
N(4)–Zn(2)–N(18)	90.1(5)	N(4)–Zn(2)–N(15)	93.2(5)
N(18)–Zn(2)–N(19)	75.1(5)	N(15)–Zn(2)–N(19)	101.4(5)

^a) Symmetry transformations used to generate equivalent atoms: #1 = $-x+2, -y, -z+1$ and #2 = $-x+1, -y, -z+1$.

$$\chi_{\text{tri}} = \frac{2N\beta^2}{KT} \frac{AA}{BB} + N\alpha \quad (1)$$

$$\chi_{\text{M}} = \chi_{\text{tri}} / [1 - \chi_{\text{tri}} (2zJ' / Ng^2 \beta^2)]$$

$$AA = g_{21}^2 + 5g_{11}^2 \exp(4J/KT) + g_{10}^2 \exp(2J/KT)$$

$$BB = 3 + 5 \exp(4J/KT) + \exp(-2J/KT) + 3 \exp(2J/KT)$$

$$g_{21} = g_{11} = \frac{g_{\text{R}}}{2} + \frac{g_{\text{Ni}}}{2}$$

$$g_{10} = g_{\text{Ni}}$$

$$N\alpha = 400 \cdot 10^{-6}$$

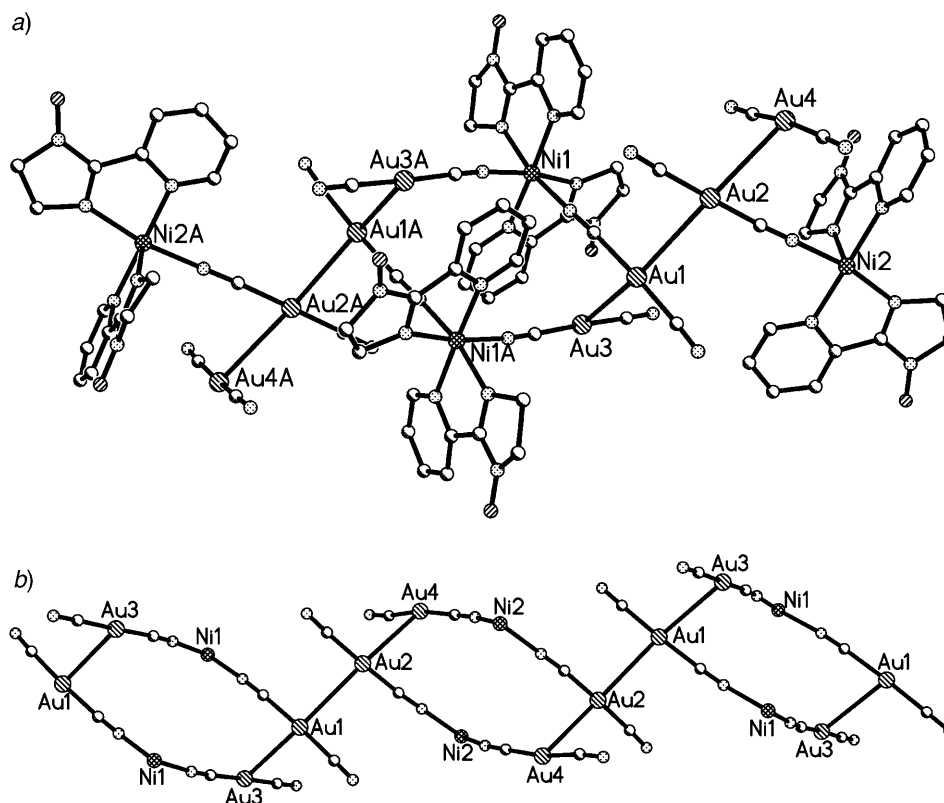


Fig. 2. a) One-dimensional zig-zag chains of complex **1** (the Me groups are omitted for clarity). b) Framework of the 1D zig-zag chains of complex **1**

Assuming $g_R = 2.00$ for complex **1**, the least-squares analysis of the magnetic susceptibility data (7–300 K) led to $g_{Ni} = 2.15$, $J = 61.8 \text{ cm}^{-1}$, $zJ' = -0.34 \text{ cm}^{-1}$, and $R = \sum[(\chi_M)_{\text{obs}} - (\chi_M)_{\text{calc}}]^2 / \sum[(\chi_M)_{\text{obs}}]^2 = 7.87 \cdot 10^{-4}$. Since one asymmetric repeat unit contains two independent $\text{Ni}(\text{tpymo})_2$ moieties, the coupling constant is the average of the actual interaction between Ni^{II} and tpymo in the two fragments. From the results, fairly large Ni^{II} –tpymo ferromagnetic interactions are observed in the present system. The strong ferromagnetic interaction is consistent with that of reported (iminomethyl nitroxide)nickel(II) complexes [36][41][42]. The ferromagnetic interaction between nickel^{II} and the iminomethyl nitroxide radical can be explained by orbital-symmetry arguments [43]. The magnetic orbital of the iminomethyl nitroxide radical has π symmetry with its axis lying perpendicular to the O–N–C–N plane. The spins of Ni^{II} reside in d_{z^2} and $d_{x^2-y^2}$, both of which have σ symmetry. Thus, all magnetic orbitals are orthogonal, which is predicted to produce ferromagnetic spin coupling. The weak intermolecular antiferromagnetic interaction (zJ') is consistent with the short intermolecular contact of uncoordinated NO groups in tpymo ligands.

Spectroscopic Properties. The absorption spectra of complexes **1** and **2** in MeCN are shown in Fig. 4, a. Compared with lanthanide/radical complexes $[\text{Ln}(\text{hfac})_3(\text{tpymo})]$

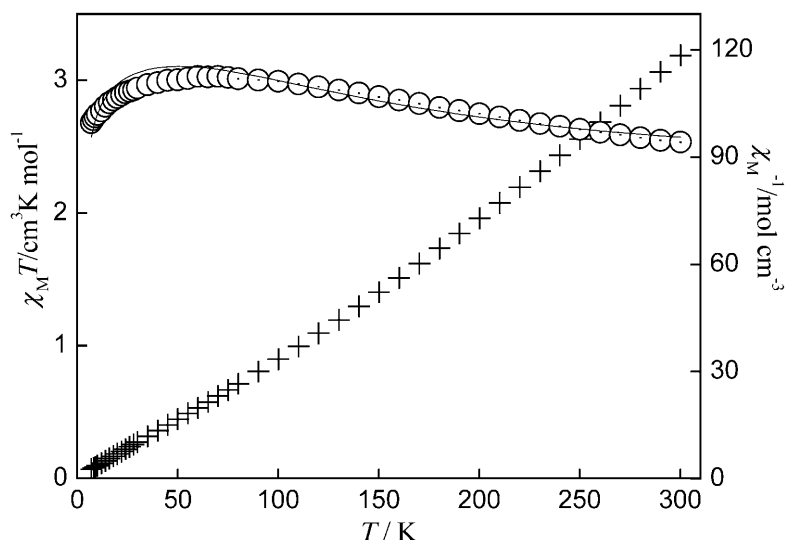


Fig. 3. Plots of $\chi_M T(\circ)$ and $\chi_M^{-1}(+)$ vs. T for complex **1**. The solid line corresponds to the best theoretical fits.

(Ln = Sm, Yb; Hhfac = 1,1,1,5,5,5-hexafluoropentane-2,4-dione) [34], the profile of the absorption spectra of **1** and **2** are very similar in the region from 410 to 530 nm, consisting of four peaks. Only a slight shift to higher frequency is observed for **2** as compared to **1**. Comparison with the intraligand $n-\pi^*$ transition of tpyimo in the corresponding region suggests to assign, the absorption bands of **1** and **2** to the intraligand $n-\pi^*$ transition, although the molar absorption coefficients for the complexes are significantly enhanced by a factor of *ca.* 10–70. This considerable increase of absorption intensities upon coordination indicates a strong interaction between tpyimo and the central metal ion.

All solid-state luminescence measurements were performed under identical conditions and instrumental parameters. Crystals of both complexes **1** and **2** show luminescence with an excitation at 260 nm at room temperature (Fig. 4, b). The profiles of the emission spectra of **1** and **2** are very similar, with four well-resolved bands around 490, 545, 590, and 613 nm, the band around 545 nm being the most intense. Comparison of the emission spectra of ligand tpyimo with those of the complexes **1** and **2** reveals no distinct change in the profiles, indicating that the luminescence spectra of **1** and **2** correspond to ligand-centered transitions. However, the emission intensity of **1** and **2** is increased with respect to that of tpyimo by a factor of *ca.* 20 for **2** and of *ca.* 2 for **1**. The cooperative effect of the bridging by the $[\text{Au}(\text{CN})_2]_4$ oligomer and the M–(tpyimo) coordination gives rise to a large enhancement of the tpyimo emission in both complexes.

The luminescent properties of Au^{I} complexes have attracted a considerable amount of attention, and the luminescence has been attributed to the presence of aurophilic interactions [17–23]. Although aurophilic interactions play a key role in the formation of the two complexes **1** and **2**, no luminescence resulting from aurophilic interactions is

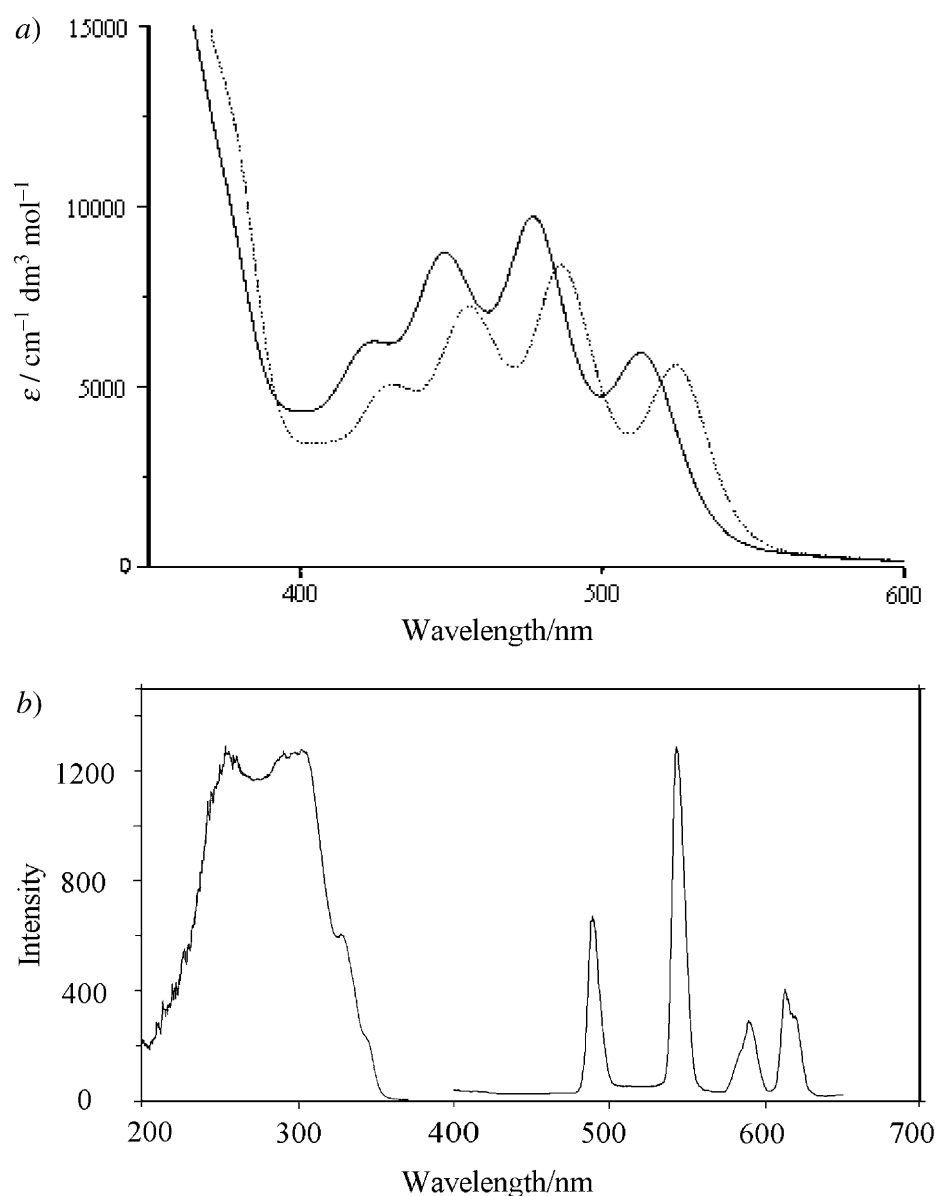


Fig. 4. a) UV/VIS Absorption spectra of **1**(\cdots) and **2**($—$) in MeCN. b) Solid-state excitation spectra (left, λ_{em} 545 nm) and emission spectra (right, λ_{ex} 260 nm) of **2** at room temperature

observed. Previous studies have shown that the luminescent energy level of the $[\text{Au}(\text{CN})_2^-]_4$ oligomer lies in the region from 420 to 440 nm [18]. Because the $n\text{-}\pi^*$ absorption band envelope for the tpyimo ligand (410–530 nm) [34] overlaps with the luminescent energy level of the $[\text{Au}(\text{CN})_2^-]_4$ oligomer, an efficient energy-transfer pro-

cess from the excited state of $[\text{Au}(\text{CN})_2^-]_4$ to tpyimo in the complexes is responsible for the complete quenching of the $[\text{Au}(\text{CN})_2^-]_4$ emissions, as shown in Fig. 5. Similar excited-state energy-transfer process has been observed previously in a $\text{Eu}[\text{Au}(\text{CN})_2^-]_3$ system [17].

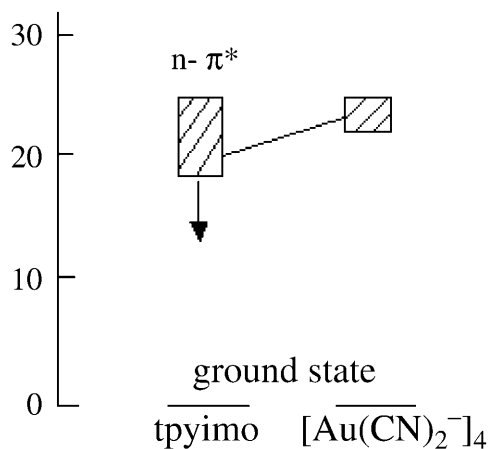


Fig. 5. Energy level diagram of the ligand tpyimo and the $[\text{Au}(\text{CN})_2^-]_4$ oligomer

Conclusion. – We prepared two novel 1-D chain complexes of an iminomethyl nitroxide radical with particular structures. The 1-D chain consists of two kinds of chair-conformation hexametal rings, in which the rings are connected to each other alternately through aurophilic interactions. On the other hand, $[\text{Au}(\text{CN})_2^-]_4$ oligomers are also formed through aurophilic interactions, and used as bridges in the 1-D chains. So the aurophilic interactions are replete with the overall structures of the complexes. The magnetic coupling between Ni^{II} and the tpyimo ligand in **1** is a strong ferromagnetic interaction. Strong ligand-centered luminescence is observed at room temperature in both complexes.

This project was supported by the *National Science Foundation of China* (No. 20331010) and the *Tianjin Natural Science Foundation* (No. 033602011).

Experimental Part

General. All chemicals were reagent grade and used without purification. Elemental analyses: *Perkin-Elmer 240* elemental analyzer. IR Spectra: *Bruker Tensor-27* FT-IR spectrometer; in the 4000–400 cm^{-1} region; KBr pellets; in cm^{-1} . Variable-temperature susceptibility measurements: *Squid-MPMS-XL7* magnetometer; temp. range 2.0–300 K at a magnetic field of 2,000 G; molar susceptibility correction from the sample holder and diamagnetic contributions of all constituent atoms by using *Pascal's* constants: *F-4500* spectrophotometer; at r.t.

4,5-Dihydro-4,4,5,5-tetramethyl-2-(pyridin-2-yl)-1H-imidazol-1-yloxy (tpyimo). The ligand tpyimo was prepared according to [44].

Bis $[\mu\text{-(cyano-}\kappa\text{C:}\kappa\text{N)}\text{tetrakis[4,5-dihydro-4,4,5,5-tetramethyl-2-(pyridin-2-yl-}\kappa\text{N)-1H-imidazol-1-yloxy-}\kappa\text{N}^3]\text{-[hexakis(cyano-}\kappa\text{C)tetrargold(3Au-Au)]dinickel}$ (**1**) and *Bis* $[\text{bis[4,5-dihydro-4,4,5,5-tetramethyl-2-(pyridin-2-yl-}\kappa\text{N)-1H-imidazol-1-yloxy-}\kappa\text{N}^3]\text{zinc}]\text{bis}[\mu\text{-(cyano-}\kappa\text{C:}\kappa\text{N)}]\text{hexakis(cyano-}\kappa\text{C)tetrargold(3Au-Au)}$ (**2**): *Caution:*

Cyanide salts are toxic and should be handled carefully! To a soln. of $M(\text{ClO}_4)_2 \cdot 6\text{H}_2\text{O}$ ($M = \text{Ni}, \text{Zn}$) (0.1 mmol) and tpyimo (0.2 mmol) in MeOH (10 ml), aq. $\text{K}[\text{Au}(\text{CN})_2]$ soln. (0.2 mmol, 5 ml) was added dropwise with stirring at r.t. After 4 h stirring, the mixture was filtered. Deep red single crystals suitable for X-ray structure analysis were grown at 279 K by the slow evaporation of the filtrate: The formulas $[\text{M}(\text{tpyimo})_2]_2[\text{Au}(\text{CN})_2]_4 \cdot 6\text{H}_2\text{O} \cdot 0.75\text{MeOH}$ were supported by elemental analysis (C, H, N). Anal. calc. for $\text{C}_{56.75}\text{H}_{79}\text{Au}_4\text{N}_{20}\text{Ni}_2\text{O}_{10.75}$ (**1**): C 32.17; H 3.76, N 13.22; found: C 32.20, H 3.79, N 13.18. Anal. calc. for $\text{C}_{56.75}\text{H}_{79}\text{Au}_4\text{N}_{20}\text{O}_{10.75}\text{Zn}_2$ (**2**): C 31.97, H 3.74, N 13.14; found: C 31.97, H 3.67, N 13.14.

X-Ray Crystallography. Crystals of dimensions $0.22 \times 0.18 \times 0.12$ mm for complex **1** and $0.38 \times 0.20 \times 0.16$ mm for complex **2** were mounted on a *Bruker Smart-1000* area detector (Mo- $K\alpha$ radiation, ϕ - ω scans) at 293(2) K. The empirical absorption corrections by SADABS were carried out. The structures were solved by direct methods and successive *Fourier* difference syntheses (SHELXS-97) [45] and refined by full-matrix least-squares procedure on F^2 with anisotropic thermal parameters for all non-H-atoms (SHELXL-97) [46]. The H atoms were located by geometry and assigned with common isotropic displacement factors and included in the final refinement by using geometrical restraints. H_2O and MeOH molecules were located from the difference *Fourier* map, whereas H-atoms of H_2O were not located from difference map and were omitted in the refinement. The thermal parameter indicates that the MeOH molecule is only partially occupied. The C(7)–N(7) of a $[\text{Au}(\text{CN})_2]^-$ anion is disordered in two positions, and the C–N distance was restrained to 1.1 Å with the occupancy factor of 0.41(4)/0.59(4) for **1** and 0.66(5)/0.34(5) for **2**. The disorder in the imidazole rings of the nitroxide ligands is not simply thermal motion but disorder caused by reverse puckering of the imidazole rings. Crystal data and details of structural determination refinement are summarized in *Table 1*. CCDC-226021 and CCDC-226020 contain the supplementary crystallographic data for **1** and **2**, respectively. These data can be obtained free of charge from the *Cambridge Crystallographic Data Centre* via http://www.ccdc.cam.ac.uk/data_request/cif.

REFERENCES

- [1] O. M. Yaghi, H. L. Li, C. Davis, D. Richardson, T. L. Groy, *Acc. Chem. Res.* **1998**, *31*, 474.
- [2] D. Braga, F. Grepioni, G. R. Desiraju, *Chem. Rev.* **1998**, *98*, 1375.
- [3] L. Ouahab, *Chem. Mater.* **1997**, *9*, 1909 and ref. cit. therein.
- [4] O. M. Yaghi, G. Li, H. Li, *Nature (London)* **1995**, *378*, 703.
- [5] O. M. Yaghi, H. Li, T. L. Groy, *J. Am. Chem. Soc.* **1996**, *118*, 9096.
- [6] O. M. Yaghi, H. Li, *J. Am. Chem. Soc.* **1995**, *117*, 10401.
- [7] O. M. Yaghi, H. Li, *J. Am. Chem. Soc.* **1996**, *118*, 295.
- [8] M. Kondo, T. Okubo, A. Asami, S. Noro, T. Yoshimoto, S. Kitagawa, T. Ishii, H. Matsuzaka, K. Seki, *Angew. Chem., Int. Ed.* **1999**, *38*, 140.
- [9] M. Fujita, Y. J. Kwon, S. Washizu, K. Ogura, *J. Am. Chem. Soc.* **1994**, *116*, 1151.
- [10] M. Kondo, T. Yoshimoto, K. Seki, H. Matsuzaka, S. Kitagawa, *Angew. Chem., Int. Ed. Engl.* **1997**, *36*, 1725.
- [11] S. Noro, S. Kitagawa, M. Kondo, K. Seki, *Angew. Chem., Int. Ed.* **2000**, *39*, 2082.
- [12] J. C. Vickery, M. M. Olmstead, E. Y. Fung, A. L. Balch, *Angew. Chem., Int. Ed. Engl.* **1997**, *36*, 1179.
- [13] V. W. W. Yam, E. C. C. Cheng, K. K. Cheung, *Angew. Chem., Int. Ed.* **1999**, *38*, 197.
- [14] Y. A. Lee, J. E. McGarrah, R. J. Lachicotte, R. Eisenberg, *J. Am. Chem. Soc.* **2002**, *124*, 10662.
- [15] R. L. White-Morris, M. M. Olmstead, F. L. Jiang, D. S. Tinti, A. L. Balch, *J. Am. Chem. Soc.* **2002**, *124*, 2327.
- [16] R. L. White-Morris, M. M. Olmstead, A. L. Balch, *J. Am. Chem. Soc.* **2003**, *125*, 1033.
- [17] Z. Assefa, G. Shankle, H. H. Patterson, R. Reynolds, *Inorg. Chem.* **1994**, *33*, 2187.
- [18] M. A. Rawashdeh-Omary, M. A. Omary, H. H. Patterson, J. P. Fackler Jr., *J. Am. Chem. Soc.* **2001**, *123*, 11237.
- [19] M. Stender, M. M. Olmstead, A. L. Balch, D. Rios, S. Attar, *Dalton Trans.* **2003**, 4282.
- [20] Z. Assefa, M. A. Omary, B. G. McBurnett, A. A. Mohamed, H. H. Patterson, R. J. Staples, J. P. Fackler Jr., *Inorg. Chem.* **2002**, *41*, 6274.
- [21] H. Schmidbaur, *Chem. Soc. Rev.* **1995**, *24*, 391.
- [22] P. Pyykkö, *Chem. Rev.* **1997**, *97*, 597.
- [23] W. Dong, L. N. Zhu, Y. Q. Sun, M. Liang, Z. Q. Liu, D. Z. Liao, Z. H. Jiang, S. P. Yan, P. Cheng, *Chem. Commun.* **2003**, 2544.
- [24] A. Caneschi, D. Gatteschi, P. Rey, R. Sessoli, *Inorg. Chem.* **1991**, *30*, 3936.
- [25] A. Caneschi, F. Ferraro, D. Gatteschi, P. Rey, R. Sessoli, *Inorg. Chem.* **1991**, *30*, 3162.

- [26] M. G. F. Vaz, L. M. M. Pinheiro, H. O. Stumpf, A. F. C. Alcântara, S. Golhen, L. Ouahab, O. Cador, C. Mathonière, O. Kahn, *Chem.–Eur. J.* **1999**, *5*, 1486.
- [27] K. Fegy, D. Luneau, T. Ohm, C. Paulsen, P. Rey, *Angew. Chem., Int. Ed.* **1998**, *37*, 1270.
- [28] L. C. Li, D. Z. Liao, Z. H. Jiang, S. P. Yan, *J. Chem. Soc., Dalton Trans.* **2002**, 1350.
- [29] H. H. Lin, S. Mohanta, C. J. Lee, H. H. Wei, *Inorg. Chem.* **2003**, *42*, 1584.
- [30] K. E. Vostrikova, D. Luneau, W. Wernsdorfer, P. Rey, M. Verdaguer, *J. Am. Chem. Soc.* **2000**, *122*, 718.
- [31] H. Oshio, M. Yamamoto, T. Ito, *Inorg. Chem.* **2002**, *41*, 5817.
- [32] L. Y. Wang, B. Zhao, C. X. Zhang, D. Z. Liao, Z. H. Jiang, S. P. Yan, *Inorg. Chem.* **2003**, *42*, 5804.
- [33] I. Dasna, S. Golhen, L. Ouahab, O. Peña, J. Guillevic, M. Fettouhi, *J. Chem. Soc., Dalton Trans.* **2000**, 129.
- [34] T. Tsukuda, T. Suzuki, S. Kaizaki, *J. Chem. Soc., Dalton Trans.* **2002**, 1721.
- [35] H. B. Zhou, S. P. Wang, W. Dong, Z. Q. Liu, Q. L. Wang, D. Z. Liao, Z. H. Jiang, S. P. Yan, P. Cheng, *Inorg. Chem.* **2004**, *43*, 4552.
- [36] Y. Yamamoto, T. Suzuki, S. Kaizaki, *J. Chem. Soc., Dalton Trans.* **2001**, 1566.
- [37] W. R. Entley, G. S. Girolami, *Science (Washington, D.C.)* **1995**, *268*, 397.
- [38] S. Ferlay, T. Mallah, R. Ouaches, P. Veillet, M. Verdaguer, *Nature (London)* **1995**, *378*, 701.
- [39] M. Verdaguer, *Science (Washington, D.C.)* **1996**, *272*, 698.
- [40] O. Sato, T. Iyoda, A. Fujishima, K. Hashimoto, *Science (Washington, D.C.)* **1996**, *272*, 704.
- [41] Y. Tsukahara, T. Kamatani, T. Suzuki, S. Kaizaki, *Dalton Trans.* **2003**, 1276.
- [42] Y. Tsukahara, T. Kamatani, A. Iino, T. Suzuki, S. Kaizaki, *Inorg. Chem.* **2002**, *41*, 4363.
- [43] O. Kahn, R. Prins, J. Reedijk, J. S. Thompson, *Inorg. Chem.* **1987**, *26*, 3557.
- [44] T. Akita, Y. Mazaki, K. Kobayashi, *J. Org. Chem.* **1995**, *60*, 2092.
- [45] G. M. Sheldrick, 'SHELXS-97. Program for X-ray Crystal Structure Determination', Göttingen University, Germany, 1997.
- [46] G. M. Sheldrick, 'SHELXL-97. Program for X-ray Crystal Structure Refinement', Göttingen University, Germany, 1997.

Received March 9, 2005